DETECTION OF A SINGLE-Λ HYPERNUCLEUS IN J-PARC E07 EXPERIMENT*

Htaik Nandar Kyaw[1], Chan Myae Aung[2]

Abstract

A single-Λ hypernucleus event which is detected in nuclear emulsion of J-PARC E07 experiment is analysed by applying relativistic kinematics. The ranges and position angles of charged particles tracks are calculated by using the position data supported by J-PARC E07 collaborators. The neutral particle emission at production point A and decay point B of single-Λ hypernucleus is checked by using the colinearity of two tracks and it is observed that, there is no neutral particle emission at point A but there is one or more neutral particles emission at point B. Charged particle track #4 is identified by its momentum and it is to be one of baryon families. The calculated results are compared with known experimental results. According to the analysis at point A, captured nucleus of Ξ^- hyperon is identified as ${}^{14}_{7}\mathrm{N}$ and the charged particle track #2 is identified as ${}^{4}_{2}\mathrm{He}$. At point B, single-Λ hypernucleus track #1 is identified as ${}^{10}_{\Lambda}\mathrm{Be}$ and charged particle track #3 and #4 are identified as ${}^{6}_{3}\mathrm{Li}$ and ${}^{1}_{1}\mathrm{H}$. In addition to charged particles emission, neutral particles are contaminated at point B.

Keywords: J-PARC E07 experiment, position data, colinearity, single-Λ hypernucleus.

Introduction

Hypernuclear Physics is the study of nuclei in which one or more hyperons are involved in addition to nucleons (protons and neutrons). Hyperons possess a new property, strangeness quantum number. Due to strangeness contamination, a lambda hyperon is free from Pauli's exclusion principle. So it can explore the nuclear matter deeply and it may give various modifications of nuclear structure such as neutron star.

At present, a lot of data have been accumulated for nucleon-nucleon (NN) interaction. However, unified understanding the baryon-baryon interaction can be obtained by considering both nucleon and hyperons. But, hyperon-nucleon and hyperon-hyperon interactions data are very scarce. So, identification of observed hypernuclei is the most important work.

To develop the field of hypernuclear physics, both theoretical and experimental researches are performing with great effort. This research work is focused on the identification of single-Λ hypernucleus event by using the emulsion scanning data of J-PARC E07 experiment.

Experimental Procedure of J-PARC E07 Experiment

J-PARC E07 experiment, which stands for Japan Accelerator Research Complex, is aimed to improve the roles of material science, life science, nuclear physics and particle physics, especially in astrophysics. J-PARC E07 experiment was performed at K 1.8 beam line in J-PARC Hadron hall.

---

* First Prize(2023)
[1] Department of Physics, Kyaukse University
[2] Departments of Physics, Defence Services Academy

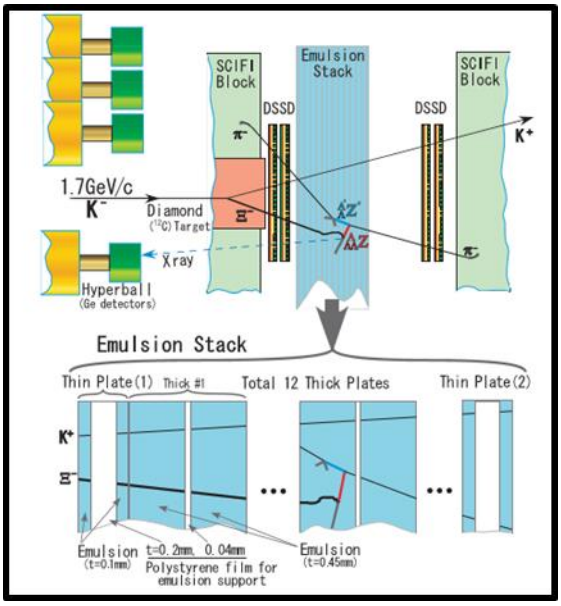

Figure1. Experimental set up of J-PARC E07 Experiment

This experiment is expected to detect approximately 100 double- Λ hypernuclear events among 10,000 Ξ^- stopping events by using hybrid emulsion method [Ekawa H, 2015]. In this experiment, the SSDs (Silicon micro-strip Detectors) and emulsion sheets are main detectors to detect hypernuclei which are the decay products of Ξ^- hyperons.

Beam exposure of J-PARC E07 was carried out in 2016 and 2017. The emulsion plates located between the two spectrometers are used to detect hypernuclei. There are 118 emulsion plates in J-PARC E07 experiment. Each emulsion plate consists of twelve thick emulsion sheets between two thin emulsion sheets. All of the thick and thin emulsion sheets are packed together in a stainless case and fixed tautly by vacuum pumping. Emulsion plates are stored in Kamioka mine located at Japan and surrounded by lead block.

In order to be able to get the exact measurement of ranges of charged particles in nuclear emulsion, it is important to know accurately the stopping power of emulsion for charged particles of various energies and thus establish the relationship between the energy of a charged particle and its range in the emulsion. The tracks of charged particles consist of a lot of silver grains with the size of about 1μm. The photograph of a nuclear emulsion is shown in figure 3.

Nuclear emulsion is a three dimensional photographic film and a high sensitive particles detector. It is used to detect the trajectories [Morishima K, 2015] of charged particles in three dimensions with submicron resolution. These trajectories are recorded as tracks formed by the ionization process. Tracks of Ξ^- hyperons are searched in first emulsion sheet by the scanning system. Then, tracks are followed in the thick-type emulsion sheets with an automatic tracking system [Soe M K, 2017] by a series of microscopic images along a predicted track. Finally, a three vertices topology found at the end point of the followed track is performed by a detailed analysis.

The Ξ^- tracks are kinematically analyzed with the SSD detector by tagging (K^-, K^+) reaction. The Ξ^- candidate tracks which are consistent with the kinematical analysis are constructed. Only the Ξ^- candidate tracks with high energy deposit in SSD detector are chosen.

These Ξ^- tracks are high stopping probability. The emitted Ξ^- candidate tracks by the emulsion module without forming nuclear reactions are rejected by the downstream SSD detector.

The Ξ^- hyperons entering the emulsion module through the SSDs are traced by an automated scanning system. When the Ξ^- hyperons are predicted, the Ξ^- tracks are searched by scanning the most upstream sheets of emulsion modules within the area of 200μm × 200μm. After the human eyes check of the tracks images by the microscope system, we determine the kinematical analysis of decay daughters and identify the nuclear process from the image information. α-tracks decay chains within the thorium series isotopes with largest rages and largest kinetic energy can be searched by an Overall Scanning Method. At present, the Overall Scanning Method is the appropriate technique to search hypernuclei and the J-PARC experiment is upgraded up to 30 GeV [Yamazaki Y, 2019] of beam energy.

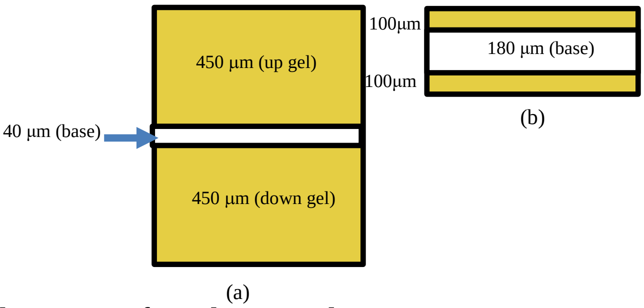

Figure 2. Schematic diagrams of nuclear emulsion in J-PARC E07 experiment; (a) thick emulsion plate and (b) thin emulsion plate

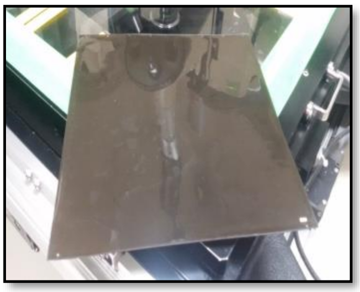

Figure 3. A photograph of a nuclear emulsion

Analysis of a Single-Λ Hypernucleus of J-PARC E07 Experiment

In this paper, a single-Λ hypernucleus event which is observed in J-PARC E07 experiment is kinematically analysed. The analysed event is detected in module #59, plate number #08 of J-PARC E07 experiment. The experimental data are provided by Professor Nakazawa and J-PARC E07 collaborators from Gifu University. Identification of hypernuclei events in nuclear emulsion has great physical interest. To perform this research work, kinematical analysis which is based on relativity theory is used. The detailed method of particles identification process will be presented in this section.

Event Description

In nuclear emulsion, a Ξ^- hyperon is captured by the emulsion nucleus at production point A from which two charged particles tracks #1 and #2 are emitted. At decay point B, track #1 decayed again into two charged particles tracks #3 and #4. This analysed event has two vertex points so that we identified as a single-Λ hypernucleus event. The photograph and schematic diagram of analyzed single-Λ hypernucleus event are presented in figure 4.

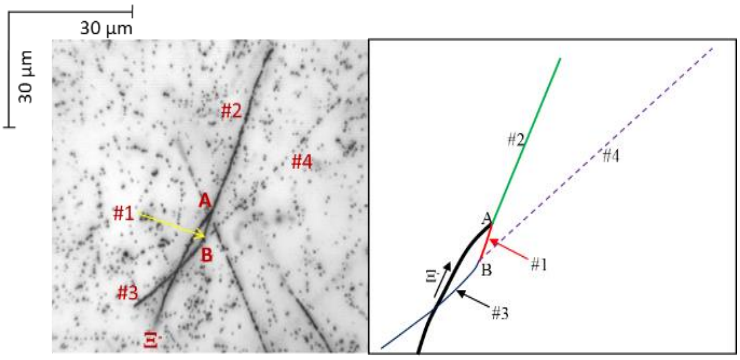

Figure 4. Photograph and schematic diagram of an analysed single-Λ hypernucleus event

Results and Discussions

Calculation of Ranges and Position Angles of Analysed Event

From experimental data, the positions (x, y, z) of tracks charged particles tracks (#1, #2, #3 and #4) were measured by three times. Using these measured data, the ranges formed by each click point for all charged particles tracks are calculated by equation (1).

Position angles of four charged particles tracks are calculated from calculated range values of these charged particles by using equation (2) and (3). The zenith angle θ is defined as the angle between a track of charged particle, range (R), and a verticle line, passing through z-direction. The azimuthal angle ϕ refers to the counter-clockwise angle from x-axis formed when the point is projected onto xy-plane. In equation (1), ‘S’ represents the shrinkage factor of emulsion plate.

$$R = \sqrt{\Delta x^2 + \Delta y^2 + (\Delta Z.S)^2} \quad (1)$$

$$\theta = \cos^{-1}\left[\frac{\Delta z}{\sqrt{\Delta x^2 + \Delta y^2 + (S.\Delta z)^2}}\right] \quad (2)$$

$$\Phi = \tan^{-1}\left[\frac{\Delta y}{\Delta x}\right] \quad (3)$$

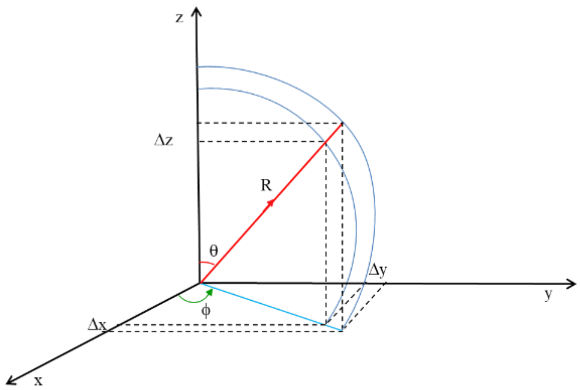

Figure 5. Schematic drawing for position angles θ and ϕ of the emitted charged particles tracks

For the first step of hypernuclei identification, ranges and position angles of four charged particles tracks are obtained from kinematical analysis as shown in table 1.

Table 1. Ranges and position angles of tracks #1, #2, #3 and #4

Vertex	Track	R (μm)	(θ) (degree)	(ϕ) (degree)
A	#1	8.33±0.005	81.67±0.59	109.53±2.74
	#2	50.17±0.006	97.35±0.55	294.59±2.45
B	#3	29.20±0.003	65.12±2.35	132.59±0.90
	#4	>13473.59±0.79	109.81±1.67	319.34±0.87

In kinematical analysis, neutral particles emission at production and decay point is necessary to check. So, we performed that neutral particle emission is where or not for both vertices. There is no neutral particles emission at production point according to collinear checking. However, there'll be neutral particles emission at decay point. Thus, one or more neutral particles emission is considered in our analysis at decay point.

Analysis at Decay Point B

At point B, possibility of mesonic and non-mesonic decay is considered to identify track #4. Due to track formation and its range, track #4 may be π^- meson. However, possibility of π^- meson has a little chance according to momentum balance checking. At point B, π^0 meson emission is impossible due to comparison of total kinetic energy and Q-values for all possible decay modes. So, track #4 is identified as a baryon (i.e proton, deuteron, triton, helium and so on). Our analysis is continued as baryon decay and 161 decay modes are obtained. Some examples of non-mesonic decay modes are shown in table 2.

Table 2. **Some examples of non-mesonic decay modes**

No.	Single-Λ Hypernucleus (Track #1)	Decay Products		
		Track #3	Track #4	Neutral Particles
1	${}^{4}_{\Lambda}He$	${}^{3}_{1}H$	${}^{1}_{1}H$	
2		${}^{2}_{1}H$	${}^{1}_{1}H$	n
3		${}^{1}_{1}H$	${}^{1}_{1}H$	2n
4	${}^{5}_{\Lambda}He$	${}^{3}_{1}H$	${}^{1}_{1}H$	n
5		${}^{2}_{1}H$	${}^{1}_{1}H$	2n

Then, kinetic energy and momenta of decay products of single-Λ hypernuclei for all possible decay modes are calculated using range-energy software package. Total kinetic energy and Q-values are also calculated and compared using equations (4) and (5).

$$Q\ (MeV) = [M_{\#1}-\{M_{\#3} + M_{\#4} + M_{neutral}\}]c^2 \times MeV/c^2 \quad (4)$$

$$KE_{tot}\ (MeV) = KE_{\#3} + KE_{\#4} + KE_{neutral} \quad (5)$$

Decay modes with Q-values negative are rejected and 35 decay modes are chosen to continue our analysis. To identify a single-Λ hypernucleus and its decay species, invariant mass, initial mass and binding energy of single-Λ hypernuclei are calculated using equations (6) and (7).

$$M_{invariant} = M_{\#3} + M_{\#4} + M_{neutral} + KE_{\#3} + KE_{\#4} + KE_{neutral} \quad (6)$$

$$M_{initial} = M_{{}^{A}_{z}X} + M_{\Lambda} \quad (7)$$

Negative binding energy values of single-Λ hypernucleus are rejected. The invariant masses and binding energies of single-Λ hypernuclei are compared with known experimental values [Bando H, 1990]. Finally, 19 single-Λ hypernuclei (${}^{4}_{\Lambda}He$, ${}^{5}_{\Lambda}He$, ${}^{6}_{\Lambda}He$, ${}^{8}_{\Lambda}He$, ${}^{6}_{\Lambda}Li$, ${}^{7}_{\Lambda}Li$, ${}^{8}_{\Lambda}Li$, ${}^{9}_{\Lambda}Li$, ${}^{9}_{\Lambda}Be$, ${}^{10}_{\Lambda}Be$, ${}^{11}_{\Lambda}B$, ${}^{12}_{\Lambda}B$, ${}^{13}_{\Lambda}B$, ${}^{12}_{\Lambda}C$, ${}^{13}_{\Lambda}C$, ${}^{14}_{\Lambda}C$, ${}^{14}_{\Lambda}N$, ${}^{15}_{\Lambda}N$ and ${}^{16}_{\Lambda}O$) can be accepted at decay point B from 27 decay modes.

Analysis at Production Point A

Our analysis is extended for production point A depending on 19 single-Λ hypernuclei from point B. At production point A, all possible production modes are considered. Ξ^- hyperon is captured by ${}^{12}_{6}C$ or ${}^{14}_{7}N$ or ${}^{16}_{8}O$ emulsion nucleus. Charged particles tracks #1 and #2 are emitted at point A and one free lambda hyperon is escaped at point A. Therefore, 53 possible production modes are obtained. Some examples of possible production modes with their decay modes are presented in table 3.

Table 3. Some examples of possible production modes

No.	Production Mode	Decay Mode
1	$\Xi^- + {}^{14}_{7}N \rightarrow {}^{4}_{\Lambda}He + {}^{10}_{4}Be + \Lambda$	${}^{4}_{\Lambda}He \rightarrow {}^{2}_{1}H + {}^{1}_{1}H + n$
2	$\Xi^- + {}^{12}_{6}C \rightarrow {}^{5}_{\Lambda}He + {}^{7}_{3}Li + \Lambda$	${}^{5}_{\Lambda}He \rightarrow {}^{3}_{1}H + {}^{1}_{1}H + n$
3	$\Xi^- + {}^{14}_{7}N \rightarrow {}^{5}_{\Lambda}He + {}^{9}_{4}Be + \Lambda$	
4	$\Xi^- + {}^{16}_{8}O \rightarrow {}^{5}_{\Lambda}He + {}^{11}_{5}B + \Lambda$	
5	$\Xi^- + {}^{12}_{6}C \rightarrow {}^{5}_{\Lambda}He + {}^{7}_{3}Li + \Lambda$	${}^{5}_{\Lambda}He \rightarrow {}^{2}_{1}H + {}^{1}_{1}H + 2n$
6	$\Xi^- + {}^{14}_{7}N \rightarrow {}^{5}_{\Lambda}He + {}^{9}_{4}Be + \Lambda$	

Q-value for all possible production modes is calculated. Furthermore, total kinetic energy of all emitted particles is calculated by using range-energy software package and kinetic energy of free lambda paticle is calculated by using momentum conservation.

$$\Xi^- + {}^{A}_{z}X \rightarrow \#1 + \#2 + \Lambda \quad (8)$$

$$Q\,(MeV) = [M_{\Xi^-} + M_c] - [M_{\#1} + M_{\#2} + M_{\Lambda}] \quad (9)$$

$$KE_{tot}\,(MeV) = KE_{\#1} + KE_{\#2} \quad (10)$$

$$B_{\Xi^-} = [M_{\Xi^-} + M_c] - [M_{\#1} + M_{\#2} + M_{\Lambda} + KE_{\#1} + KE_{\#2}] \quad (11)$$

Table 4. Q-value, (KE_{tot}) and (B_{Ξ^-}) for some possible production modes

Production Mode	Q-value (MeV)	KE_{tot} (MeV)	B_{Ξ} (MeV)
$\Xi^- + {}^{14}_{7}N \rightarrow {}^{4}_{\Lambda}He + {}^{10}_{4}Be + \Lambda$	22.06±0.25	29.14±0.00	-7.08±0.26
$\Xi^- + {}^{12}_{6}C \rightarrow {}^{5}_{\Lambda}He + {}^{7}_{3}Li + \Lambda$	6.50±0.25	18.71±0.00	-12.21±0.25
$\Xi^- + {}^{14}_{7}N \rightarrow {}^{5}_{\Lambda}He + {}^{9}_{4}Be + \Lambda$	12.93±0.25	28.24±0.00	-15.32±0.26
$\Xi^- + {}^{16}_{8}O \rightarrow {}^{5}_{\Lambda}He + {}^{11}_{5}B + \Lambda$	8.01±0.25	38.68±0.01	-30.67±0.26
$\Xi^- + {}^{12}_{6}C \rightarrow {}^{5}_{\Lambda}He + {}^{7}_{3}Li + \Lambda$	49.11±0.26	18.71±0.00	30.39±0.26
$\Xi^- + {}^{14}_{7}N \rightarrow {}^{5}_{\Lambda}He + {}^{9}_{4}Be + \Lambda$	55.53±0.26	28.24±0.00	27.29±0.26

At production point A, the nuclear process takes place energetically so that Q-values of this process should be positive. So, 15 possible production modes with negative Q-values and 6 production modes with negative B_{Ξ^-} are rejected and 32 possible production modes are accepted.

Range estimation of charged particle track #4 is continued by comparing with assigned particles. Charged particle track #4 passes through plate number #08 to #02. Therefore, it is not stopped in emulsion plate #02. Because of this fact, stopping point of track #4 is not seen between emulsion plate #02 and #08. That's why, its range must be longer than measured range.

So, estimated range of track #4 needs to be considered. If estimated range of track #4 is shorter than measured range, it is impossible to assign the charged particle track #4. If estimated range of track #4 is very longer than measured range of it, it is also impossible to assign the charged particle track #4. So, estimated range of track #4 should be comparable with measured range of it.

Moreover, it is assumed that track #3 and track #4 is back to back direction emission at decay point. The charged particle track #4 is assigned to be a pi-minus meson, proton, deuteron or triton. Charged particle track #3 is assigned to be ${}^{1}_{1}\mathrm{H}$, ${}^{2}_{1}\mathrm{H}$, ${}^{3}_{1}\mathrm{H}$, ${}^{3}_{2}\mathrm{He}$, ${}^{4}_{2}\mathrm{He}$, ${}^{6}_{3}\mathrm{Li}$, ${}^{7}_{3}\mathrm{Li}$, ${}^{9}_{4}\mathrm{Be}$, ${}^{10}_{4}\mathrm{Be}$, ${}^{10}_{5}\mathrm{B}$, ${}^{11}_{5}\mathrm{B}$, ${}^{12}_{6}\mathrm{C}$ or ${}^{12}_{6}\mathrm{C}$. Range of track #3 is 29.20 µm. Using its range, kinetic energy of track #3 is calculated from range-energy relation. Using its kinetic energy, range of track #4 is estimated by energy-range relation software package.

$$KE_{\#4} = \frac{p_{\#4}^{2}}{2M_{\#4}} \qquad (12)$$

The estimated ranges of charged particle track #4 are compared with calculated ranges of it. The calculated range of charged particle track #4 is 13479.59 µm. Only 5 production modes with their decay modes are acceptable as shown in table 4. That's why the estimated ranges of other 27 production modes are very smaller than the calculated ranges.

Table 5. **The most acceptable possible production modes with their decay modes**

Production Mode	Decay Mode	Estimated range of #4 (µm)
$\Xi^{-} + {}^{14}_{7}\mathrm{N} \rightarrow {}^{10}_{\Lambda}\mathrm{Be} + {}^{4}_{2}\mathrm{He} + \Lambda$	${}^{10}_{\Lambda}\mathrm{Be} \rightarrow {}^{6}_{3}\mathrm{Li} + {}^{1}_{1}\mathrm{H} + 3\mathrm{n}$	17427
$\Xi^{-} + {}^{14}_{7}\mathrm{N} \rightarrow {}^{11}_{\Lambda}\mathrm{B} + {}^{3}_{1}\mathrm{H} + \Lambda$	${}^{11}_{\Lambda}\mathrm{B} \rightarrow {}^{9}_{4}\mathrm{Be} + {}^{2}_{1}\mathrm{H}$	13899
$\Xi^{-} + {}^{14}_{7}\mathrm{N} \rightarrow {}^{12}_{\Lambda}\mathrm{B} + {}^{2}_{1}\mathrm{H} + \Lambda$	${}^{12}_{\Lambda}\mathrm{B} \rightarrow {}^{10}_{4}\mathrm{Be} + {}^{2}_{1}\mathrm{H}$	17485
$\Xi^{-} + {}^{16}_{8}\mathrm{O} \rightarrow {}^{12}_{\Lambda}\mathrm{B} + {}^{4}_{2}\mathrm{He} + \Lambda$	${}^{13}_{\Lambda}\mathrm{C} \rightarrow {}^{11}_{5}\mathrm{B} + {}^{2}_{1}\mathrm{H}$	17485
$\Xi^{-} + {}^{16}_{8}\mathrm{O} \rightarrow {}^{13}_{\Lambda}\mathrm{C} + {}^{3}_{1}\mathrm{H} + \Lambda$		34160

Results at Production Point A

Analysis at production point is performed to consistence at decay point B. According to our analysis at production point and decay point, the captured nuclei are accepted as ${}^{14}_{7}\mathrm{N}$ or ${}^{16}_{8}\mathrm{O}$. The single-Λ hypernucleus track #1 is accepted as ${}^{10}_{\Lambda}\mathrm{Be}$ or ${}^{11}_{\Lambda}\mathrm{Be}$ or ${}^{12}_{\Lambda}\mathrm{Be}$ or ${}^{13}_{\Lambda}\mathrm{C}$. The most acceptable production modes with their respective decay modes are presented in table 5.

Estimated ranges of acceptable production modes are longer than that of calculated and measured ranges and comparable with calculated range of charged particle track #4

.

Table 6. **The calculated Q-value, total kinetic energy and binding energy for possible production modes**

Production Mode	Q-value (MeV)	KE_{tot} (MeV)	B_{Ξ^-} (MeV)
$\Xi^- + {}^{14}_{7}N \rightarrow {}^{10}_{\Lambda}Be + {}^{4}_{2}He + \Lambda$	17.10 ±0.21	9.64 ±0.00	7.46 ±0.21
$\Xi^- + {}^{14}_{7}N \rightarrow {}^{11}_{\Lambda}B + {}^{3}_{1}H + \Lambda$	69.41 ±0.00	4.07 ±0.00	65.34 ±0.01
$\Xi^- + {}^{14}_{7}N \rightarrow {}^{12}_{\Lambda}B + {}^{2}_{1}H + \Lambda$	69.49 ±0.16	3.61 ±0.00	65.88 ±0.17
$\Xi^- + {}^{16}_{8}O \rightarrow {}^{12}_{\Lambda}B + {}^{4}_{2}He + \Lambda$	72.60 ±0.16	9.58 ±0.00	63.02 ±0.17
$\Xi^- + {}^{16}_{8}O \rightarrow {}^{13}_{\Lambda}C + {}^{3}_{1}H + \Lambda$	57.74 ±0.00	4.01 ±0.00	53.73 ±0.01

The charged particle track #2 is accepted as ${}^{2}_{1}H$ or ${}^{3}_{1}H$ or ${}^{4}_{2}He$. The charged particle track #3 is accepted as ${}^{6}_{3}Li$ or ${}^{9}_{4}Be$ or ${}^{10}_{4}Be$ or ${}^{11}_{5}B$. The charged particle track #4 is accepted as ${}^{1}_{1}H$ or ${}^{2}_{1}H$. From the most acceptable 5 production modes with their respective decay modes, only one production mode is identified. Because only two charged particles are emitted at decay point B for the other 4 production modes. If only charged particle is emitted at the decay point, Q-value and KE_{tot} should be comparable. But, Q-values are greater than KE_{tot} at the other 4 decay modes. So, these decay modes are rejected. Finally, the captured nucleus is identified as ${}^{14}_{7}N$ at production point A. The charged particle track #2 is identified as ${}^{4}_{2}He$ at production point A.

Results at Decay Point B

At decay point B, we accepted four decay modes depending on five production modes. For those four decay modes, Q-value and total kinetic energy for decay species are compared. Furthermore, invariant mass and known experimental mass of single-Λ hypernucleus track #1 are compared. Moreover, binding energy of single-Λ hypernucleus is also calculated and compared with known experimental binding energy. At the end of our analysis, we can identify only one decay modes at point B as ${}^{10}_{\Lambda}Be \rightarrow {}^{6}_{3}Li + {}^{1}_{1}H + 3n$. So, the single-Λ hypernucleus track #1 is identified as ${}^{10}_{\Lambda}Be$ at point B and the charged particle track #3 is identified as ${}^{6}_{3}Li$ at that point. The charged particle track #4 is identified as proton (${}^{1}_{1}H$) from decay point. At decay point B, single-Λ hypernucleus ${}^{10}_{\Lambda}Be$ decay into two charged particles (${}^{6}_{3}Li$ and ${}^{1}_{1}H$) with contamination of three neutrons. Particles identification of this research is summarized in table 7.

Table 7. Particles identification at production point A and decay point B

Production point A			**Decay point B**		
Captured nucleus	**Track #2**	**Track #1 (Single-Λ hypernucleus)**	**Track #3**	**Track #4**	**Neutral particles**
${}^{14}_{7}N$	${}^{4}_{2}He$	${}^{10}_{\Lambda}Be$	${}^{6}_{3}Li$	${}^{1}_{1}H$	3 n

Q-value is 138.78±0.0.23 MeV, total kinetic energy of decay species is >143.78±0.01 MeV and, invariant mass, initial mass, known experimental mass, binding energy and known experimental binding energy of single-Λ hypernucleus ${}^{10}_{\Lambda}Be$ are > 9504.31±0.21 MeV/c^2, 9510.48±0.00 MeV/c^2, 9499.33±0.23 MeV/c^2 , < 6.71±0.21 MeV and 9.11±0.22 MeV.

Conclusion

The main purposes of strangeness hypernuclear physics are to extend the strangeness nuclear chart and to understand the structures of multi-strangeness systems. Therefore, the basic concepts of the hypernuclear physics are studied and collaborated in the hypernuclear experiments.

Present research work is focused on the identification of single-Λ hypernucleus event by using the emulsion scanning data of J-PARC E07 experiment. According to the decay topology of this event, a single-Λ hypernucleus event is firstly identified. But the kinematical analysis is inevitably needed to identify this event. That's why, present analysis is performed starting from range calculation to binding energy calculation of a single-Λ hypernucleus.

In this work, the ranges and position angles of the analysed event were calculated by using the experimental data from J-PARC E07 experiment. A single-Λ hypernucleus event can be identified by its decay topology and the decay daughters of a single-Λ hypernucleus have to be known. So, possible mesonic or non-mesonic decays are considered and checking the possibility of track #4 is the main analysis of particle identification.

From the present research, it can be obtained useful information for Λ-N interaction. Hypernuclear physics is now developing and it is necessary to get more and more information and data on hypernuclear production, decay, life time, mass and binding energy, etc. The present research can support those data to hypernuclear physics group.

Acknowledgements

I would like to thank Professor Nakazawa, Head of Physics Department, Gifu University, and all collaborators of J-PARC E07 experiment for their discussions, supports and valuable advices to carry out hypernuclear research.

References

Bando H, Motoba T and Zofka J (1990), "Production, Structure and Decay of Hypernuclei", *International Journal of Modern Physics A*, Vol. 5, pp 4021-4198.

Ekawa H et al., (2015), "Observation of a $_{\Lambda\Lambda}$Be double-Λ hypernucleus in the J-PARC E07 experiment," *Prog. Theor. Exp. Phys*. DOI: 10.1093/ptep/0000000000.

Morishima K (2015), "Latest Developments in Nuclear Emulsion Technology," 26th International Conference on Nuclear Tracks in Solids, 26ICNTS, *Physics Procedia* 80 pp 19-24.

Soe M K, et al.(2017), Nucl. Instrum. Methods Phys. Res. Sect. A 848, pp 66-72.

Yamazaki Y, J-PARC, KEK and JAEA, Japan (2020), "From KEK-PS To J-PARC."